GENE EDITING

In utero gene editing for monogenic lung disease

Deepthi Alapati[1,2,3,4,5], William J. Zacharias[3,4,5,6], Heather A. Hartman[7], Avery C. Rossidis[7], John D. Stratigis[7], Nicholas J Ahn[7], Barbara Coons[7], Su Zhou[3,5], Hiaying Li[7], Kshitiz Singh[7], Jeremy Katzen[3,4], Yaniv Tomer[3,4], Alexandra C. Chadwick[3,5], Kiran Musunuru[3,5], Michael F. Beers[3,4], Edward E. Morrisey[3,4,5]*, William H. Peranteau[7]*

Monogenic lung diseases that are caused by mutations in surfactant genes of the pulmonary epithelium are marked by perinatal lethal respiratory failure or chronic diffuse parenchymal lung disease with few therapeutic options. Using a CRISPR fluorescent reporter system, we demonstrate that precisely timed in utero intra-amniotic delivery of CRISPR-Cas9 gene editing reagents during fetal development results in targeted and specific gene editing in fetal lungs. Pulmonary epithelial cells are predominantly targeted in this approach, with alveolar type 1, alveolar type 2, and airway secretory cells exhibiting high and persistent gene editing. We then used this in utero technique to evaluate a therapeutic approach to reduce the severity of the lethal interstitial lung disease observed in a mouse model of the human *SFTPC*^{I73T} mutation. Embryonic expression of *Sftpc*^{I73T} alleles is characterized by severe diffuse parenchymal lung damage and rapid demise of mutant mice at birth. After in utero CRISPR-Cas9–mediated inactivation of the mutant *Sftpc*^{I73T} gene, fetuses and postnatal mice showed improved lung morphology and increased survival. These proof-of-concept studies demonstrate that in utero gene editing is a promising approach for treatment and rescue of monogenic lung diseases that are lethal at birth.

INTRODUCTION

Congenital genetic lung diseases, such as inherited surfactant protein (SP) syndromes, cystic fibrosis, and alpha-1 antitrypsin deficiency, are a source of morbidity and mortality for which no definitive treatment options exist (*1*–*4*). These disorders present with a spectrum of severity and timing of onset. Some, such as cystic fibrosis and alpha-1 antitrypsin deficiency, present in late childhood or early adulthood with subsequent disease progression and shortened life expectancy (*5*, *6*). Alternatively, mutations in SP genes can cause respiratory failure at birth and perinatal death or chronic diffuse lung disease. Genetic mutations in one of three surfactant system genes, *SFTPB*, *SFTPC*, or *ABCA3* (adenosine triphosphate–binding cassette protein member 3), result in either a loss-of-function phenotype through disruption of surfactant metabolism or its biophysical activity (SP deficiency syndrome) or a toxic gain-of-function phenotype from disrupted lung development or diffuse parenchymal lung disease perpetrated by cytosolic accumulation of abnormal SP conformers in alveolar type 2 (AT2) cells. Heterozygous mutations in *SFTPC* are a primary cause of children's interstitial lung disease (chILD). The age of onset and severity of disease due to *SFTPC* mutations depend on the specific mutation and vary from severe respiratory failure in neonates to idiopathic pulmonary fibrosis in adulthood (*7*, *8*). Unlike surfactant deficiency of prematurity, the inherited forms of SP disease do not respond to exogenous surfactant, anti-inflammatory, or antifibrotic therapies. Treatment options for patients presenting with neonatal respiratory failure are limited to palliative care or pediatric lung transplant, which is limited by organ availability (*9*, *10*). Thus, there is an urgent need for therapies for early correction of lethal genetic lung disorders including SP syndromes.

Recent improvements in gene editing technology, including advances in CRISPR-Cas9 [clustered regularly interspaced short palindromic repeats (CRISPR)–CRISPR-associated 9] technology, offer an unprecedented opportunity for therapeutic correction of monogenic disorders (*11*–*15*). Standard CRISPR-Cas9 gene editing uses a single-guide RNA (sgRNA) to instigate a double-strand DNA break (DSB) in a site-specific fashion. Normal cellular mechanisms repair the DSB via nonhomologous end joining (NHEJ), or if a donor repair template is provided, then homology-directed repair can be accomplished at low efficiency. Studies in postnatal mouse models have demonstrated the therapeutic potential of in vivo CRISPR-Cas9 gene editing to correct monogenic diseases (*16*–*21*).

Although postnatal in vivo gene editing studies are encouraging (*16*–*21*), some diseases, such as SP syndromes, result in morbidity and mortality at the time of or shortly after birth, precluding a postnatal approach. Several examples of early zygote gene editing have been described and could prove useful where mutation detection at very early developmental time points is possible (*22*–*24*). However, de novo mutations that occur later in development may not be treatable by early zygote gene editing. Using CRISPR-Cas9 gene editing to correct lung diseases during later prenatal developmental stages has the potential to reverse such genetic abnormalities before transition to postnatal life when pulmonary function becomes essential. In utero gene editing also provides the opportunity to take advantage of the normal developmental properties of the fetus to accomplish efficient gene editing. Specifically, the small size and immunologic immaturity of the fetus allow for the optimization of the CRISPR-Cas9 "dose" per recipient weight while avoiding a potential immune response to the bacterial Cas9 protein or delivering viral vector (*25*–*28*). In addition, the target cell population for

[1]Department of Pediatrics Nemours, Alfred I duPont Hospital for Children, Wilmington, DE 19803, USA. [2]Department of Pediatrics Sidney Kimmel Medical College, Thomas Jefferson University Philadelphia, Philadelphia, PA 19107, USA. [3]Department of Medicine, Perelman School of Medicine at the University of Pennsylvania, Philadelphia, PA 19104, USA. [4]Penn Center for Pulmonary Biology, Perelman School of Medicine at the University of Pennsylvania, Philadelphia, PA 19104, USA. [5]Penn Cardiovascular Institute, Perelman School of Medicine at the University of Pennsylvania Philadelphia, Philadelphia, PA 19104, USA. [6]Division of Pulmonary Biology Cincinnati Children's Hospital, Department of Pediatrics University of Cincinnati College of Medicine, Cincinnati, OH 45529, USA. [7]Center for Fetal Research, Division of General, Thoracic, and Fetal Surgery, Children's Hospital of Philadelphia, Philadelphia, PA 19104, USA. *Corresponding author. Email: emorrise@pennmedicine.upenn.edu (E.E.M.); peranteauw@email.chop.edu (W.H.P.)

gene editing may be more accessible in the fetus. In the postnatal lung, immune and physical barriers including mucus and glycocalyx proteins limit access to pulmonary epithelial cells including AT2 cells, the target cell population for SP disorders (*29*, *30*). These immune and physical barriers are not as formidable in the fetus, and multiple murine studies have demonstrated efficient gene transfer to pulmonary epithelial cells after prenatal viral vector delivery via intra-amniotic injection to take advantage of fetal breathing movements for lung targeting (*31*–*33*).

In the current study, we demonstrate the feasibility, efficiency, and specificity of prenatal CRISPR-Cas9–mediated gene editing of the lung in two mouse models. We first developed a targeting strategy for a commercially available fluorescent reporter mouse model (*34*), to demonstrate efficient and persistent gene editing, and found that our approach predominantly restricted gene editing to pulmonary epithelial cells after intra-amniotic delivery of CRISPR-Cas9 reagents. We then evaluated the therapeutic role of fetal lung gene editing using a mouse model expressing a chILD-causing mutation, *Sftpc*^{I73T} (*35*). When expressed in mice during embryogenesis, the SP-C^{I73T} proprotein arrests lung development, causing rapid perinatal death. We show that CRISPR-Cas9–induced excision of the mutant *Sftpc*^{I73T} gene can rescue the lung from toxic accumulation of the disease-associated protein and improve lung development in *Sftpc*^{I73T} mutant mice, increasing their survival. Our proof-of-concept study demonstrates that in utero gene editing provides a therapeutic approach for the treatment of congenital lung diseases caused by defects in the pulmonary epithelium.

RESULTS

Intra-amniotic delivery of CRISPR-Cas9 results in efficient pulmonary gene editing

We initially sought to establish a model to define the efficiency and persistence of prenatal lung gene editing that could be easily monitored and quantified. Gt(ROSA)26Sor$^{tm4(ACTB-tdTomato,-EGFP)Luo}$ mice (referred to as *R26*^{mTmG}) have a two-color fluorescent cassette [mT-tdTomato: cell membrane–bound, red; mG–enhanced green fluorescent protein (EGFP): cell membrane–bound, green]that can be differentially activated by Cre recombinase (*34*). mT-tdTomato red fluorescence is constitutively expressed in the plasma membrane of all cells, including pulmonary epithelial, endothelial, and mesenchymal cells. Upon Cre expression, the mT-tdTomato complementary DNA (cDNA) along with a transcriptional stop cassette is deleted, and the mG-EGFP cassette is subsequently expressed. We chose *Streptococcus pyogenes* Cas9 (SpyCas9) to perform in utero CRISPR-Cas9 gene editing because SpyCas9 remains the most efficient version of the enzyme. Because of the large size of SpyCas9 (~4.2 kb), we chose an adenovirus (Ad) to deliver this enzyme to the developing fetus. As previous work has demonstrated that fetal breathing movements combined with theophylline and mild maternal hypercarbia treatment to stimulate respiratory drive can promote efficient and fairly specific delivery of viral vectors into the fetal lung after intra-amniotic injection (*32*, *33*), we delivered Ad vectors containing SpyCas9 and an sgRNA targeting the loxP sites flanking the mT/stop cassette (Ad.mTmG) into the amniotic cavity of gestational day (E) 16 *R26*$^{mTmG/+}$ fetuses (Fig. 1A, fig. S1A, movie S1, and table S1). Injected fetuses were assessed for editing at E19 (Fig. 1B). Control fetuses were injected with either an Ad vector containing Cre recombinase (Ad.Cre; positive control) or an Ad vector containing SpyCas9 and no sgRNA (Ad.Null). Fetuses injected with Ad.Cre and Ad.mTmG underwent extensive pulmonary gene editing, as supported by the presence of membrane-bound EGFP$^+$ cells lining both the proximal airways and distal saccules. In contrast, fetuses injected with Ad.Null lacked the expression of membrane-bound EGFP (Fig. 1, C and D). Polymerase chain reaction (PCR) analysis of genomic DNA from lungs of injected fetuses supported efficient gene editing with excision of the mT/stop cassette and subsequent NHEJ using Ad.mTmG (Fig. 1E). DNA Sanger sequencing revealed that the edited sequence contained insertions and deletions (indels) in the recombined loxP region beginning three nucleotides 5′ to the protospacer adjacent motif (PAM) site (Fig. 1F). In contrast, indels were absent in the Cre-mediated recombined loxP site (Fig. 1G). In addition to the lung, rare clusters of EGFP$^+$ edited cells and PCR analysis consistent with editing were noted in the stomach, consistent with previous studies demonstrating transduction of the proximal gastrointestinal tract after intra-amniotic Ad injection (fig. S1, B and C) (*33*). Gene editing was not detected by PCR or immunohistochemistry (IHC) in the heart, liver, skin, brain, and gonads. These data are further supported by the restricted delivery and expression of the Ad vector to the lung at this developmental time point (fig. S1D). Thus, intra-amniotic delivery of Ad vectors carrying CRISPR-Cas9 results in pulmonary gene editing.

Intra-amniotic CRISPR-Cas9 delivery targets pulmonary epithelial cells for gene editing

Because various lung epithelial cell types are affected in congenital monogenic lung diseases, we evaluated the efficiency of gene editing in individual pulmonary cell lineages (epithelial, endothelial, and mesenchymal cells) using the *R26*$^{mTmG/+}$ model. The distribution of EGFP$^+$ cells was confined to the epithelial lining throughout the lung section with sparing of the blood vessels and subepithelial regions (fig. S2A). Using flow cytometry, we quantified the fraction of pulmonary epithelial (CD45$^-$/DAPI$^-$/EPCAM$^+$), endothelial (CD45$^-$/DAPI$^-$/CD31$^+$), and mesenchymal cells (CD45$^-$/DAPI$^-$/EPCAM$^-$/CD31$^-$) that were EGFP$^+$, and thus edited, in the *R26*$^{mTmG/+}$ model just before birth at E19 (Fig. 2A and fig. S2B). EPCAM$^+$ (epithelial cell adhesion molecule) epithelial cells had the highest percentage (18%) of gene-edited cells (Fig. 2B). The Ad.Cre control showed a similar distribution of EGFP$^+$ live pulmonary cell types. The percentage of EGFP$^+$EPCAM$^+$ cells was not significantly different in the Ad.Cre group compared to the Ad.mTmG group ($P = 0.08$) (Fig. 2B). To confirm the cell type–specific efficiency of gene editing in the lung, genomic DNA from fluorescence-activated cell sorting (FACS) of isolated epithelial, endothelial, and mesenchymal cells was assessed by PCR. Consistent with the flow cytometry data, the gene-edited 545-bp band was amplified in DNA from epithelial cells but not from endothelial or mesenchymal cells from lungs of mice prenatally injected with Ad.mTmG or Ad.Cre (fig. S3, A to C).

We next assessed the efficiency of gene editing in several important lung epithelial lineages including AQP5$^+$ (aquaporin 5) alveolar epithelial type 1 (AT1) cells, SFTPC$^+$ (surfactant protein C) AT2 cells, SCGB1A1$^+$ (secretoglobin family 1A member 1) secretory airway epithelial cells, and FOXJ1$^+$ (forkhead box J1) ciliated airway epithelial cells (Fig. 2C). This analysis demonstrated that gene editing occurred in all epithelial cell subpopulations including AT2 cells, the target cell population for SP disease, and other congenital lung diseases (Fig. 2D). The distribution of gene-edited pulmonary epithelial cell subpopulations was similar to that seen in Ad.Cre-injected fetuses (Fig. 2, C and E). Membrane-bound EGFP$^+$ cells were not detected in Ad.Null-injected

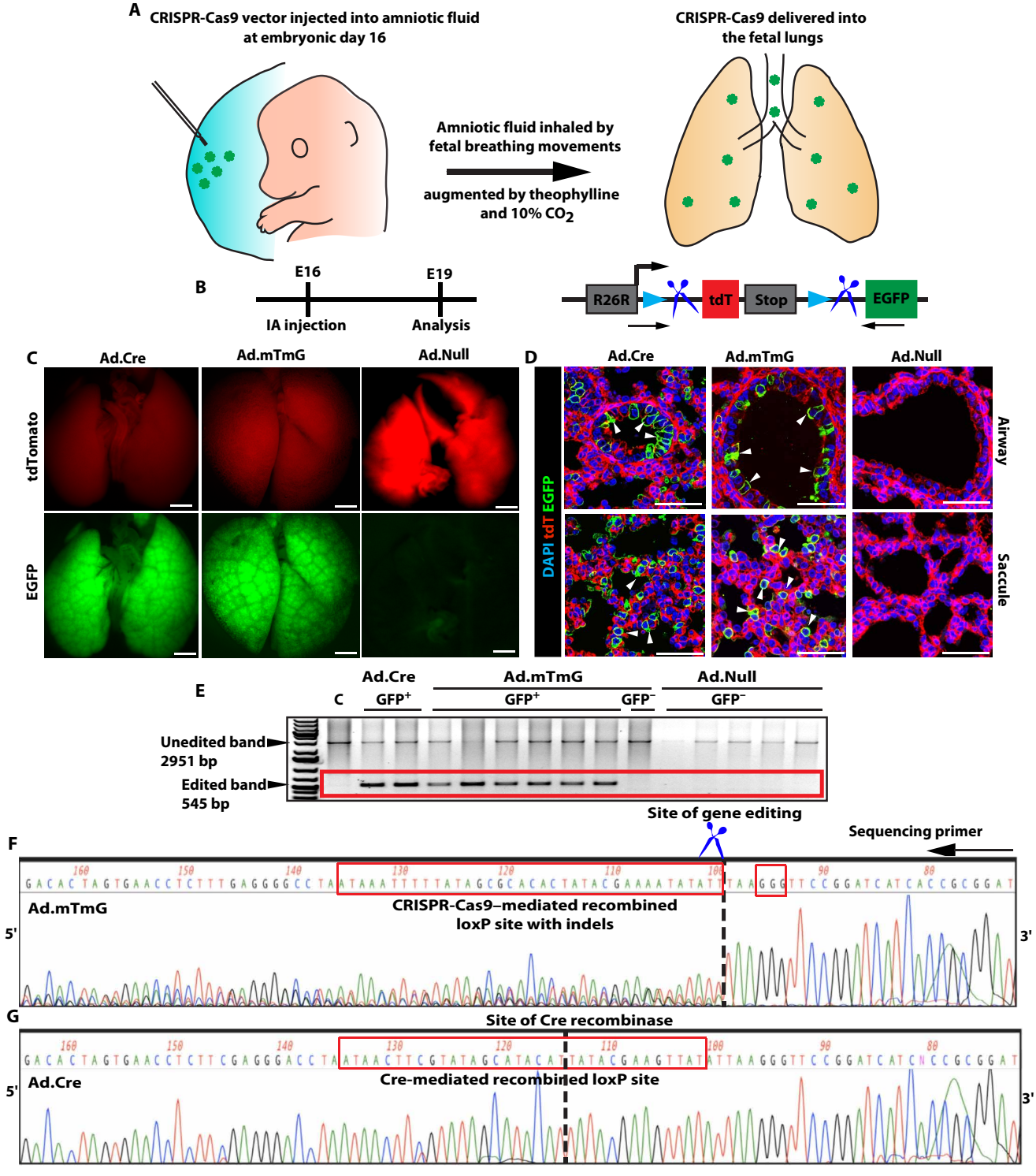

Fig. 1. Intra-amniotic delivery of CRISPR-Cas9 results in pulmonary gene editing. (**A**) Schematic representation of intra-amniotic route of fetal lung gene editing. (**B**) Experimental design of gene editing in *R26*$^{mTmG/+}$ mice. (**C**) Fluorescent stereomicroscopy, using a filter to detect tdTomato and EGFP, of lungs from *R26*$^{mTmG/+}$ mice injected with Ad.Cre, Ad.mTmG, or Ad.Null. (**D**) IHC for EGFP and tdTomato expression in the proximal airway and distal air saccules of lungs from *R26*$^{mTmG/+}$ mice injected with Ad.Cre, Ad.mTmG, or Ad.Null. White arrowheads indicate EGFP staining. (**E**) PCR assay using primers to detect the on-target editing in DNA isolated from E19 lungs of *R26*$^{mTmG/+}$ mice injected with Ad.Cre, Ad.mTmG, or Ad.Null. Edited band, 545 base pairs (bp); unedited band, 2951 bp. $n = 2$ to 6 per group. One fetus that was injected with Ad.mTmG and lacked notable EGFP fluorescence (GFP^{-}) was also negative for gene editing by PCR, indicating a likely technical failure at the time of injection. (**F**) Sanger sequencing of the 545-bp edited mTmG PCR product from an *R26*$^{mTmG/+}$ mouse injected with Ad.mTmG. (**G**) Sanger sequencing of the 545-bp Cre-recombined mTmG PCR product from an *R26*$^{mTmG/+}$ mouse injected with Ad.Cre. Scale bars, 1000 μm (C) and 50 μm (D). IA, intra-amniotic; E, gestational day.

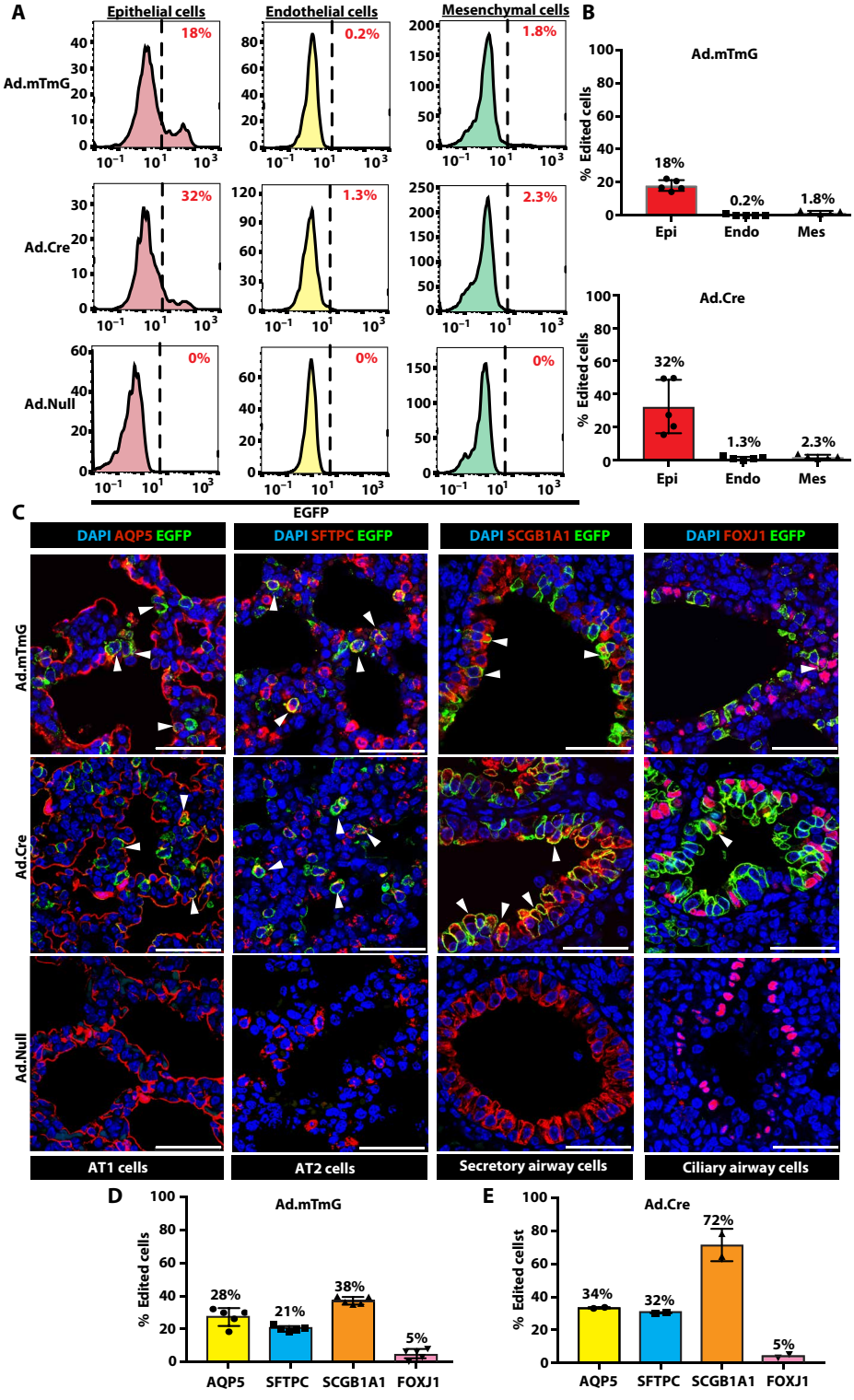

Fig. 2. Intra-amniotic delivery of CRISPR-Cas9 targets pulmonary epithelial cells for gene editing. (**A**) FACS plots of lungs harvested at E19 after intra-amniotic injection of Ad.mTmG, Ad.Cre, or Ad.Null at E16. Each row shows representative FACS plots from a single lung. (**B**) Quantitation of cell type–specific gene editing using FACS analysis for EGFP$^+$ cells within each major pulmonary cell type after intra-amniotic injection of Ad.mTmG and Ad.Cre. $n = 5$ per group. (**C**) EGFP$^+$ gene-edited and Cre-recombined cells depicted by white arrowheads within subsets of pulmonary epithelial cells marked by AQP5, SFTPC, SCGB1A1, and FOXJ1. (**D**) Quantification of gene-edited airway and alveolar epithelial cells after Ad.mTmG intra-amniotic delivery. (**E**) Quantification of Cre-recombined airway and alveolar epithelial cells after Ad.Cre intra-amniotic delivery. $n = 2$ to 5 per group. Epi, epithelial; Endo, endothelial; Mes, mesenchymal. Scale bars, 50 μm.

fetuses, pointing to the lack of spurious EGFP expression in nonedited cells and the specificity of this marker for gene editing in our model (Fig. 2C). Last, a recent study suggests the possibility of large unwanted deletions or complex rearrangements after CRISPR-Cas9 gene editing (*36*). The $R26^{mTmG/+}$ model provides an elegant system in which to assess for this event. Specifically, an unwanted large deletion at the $R26^{mTmG}$ allele would likely inactivate both the mT and mG fluorescent reporters, resulting in $EGFP^{-}tdT^{-}$ cells. Analysis of $EPCAM^{+}$ cells did not demonstrate an increase in the double-negative cell population in the lungs of Ad.mTmG-injected compared to Ad.Cre-injected mice, suggesting that this event did not occur above background levels (fig. S3D).

Pulmonary epithelial cell editing is stable after prenatal CRISPR delivery

Although the lung is considered to be a fairly quiescent organ, there is a slow steady-state turnover of cells in the postnatal period. Using the $R26^{mTmG/+}$ model, we assessed the persistence of gene-edited pulmonary cells over time using flow cytometry and IHC at E19, postnatal day (P) 7, P30, and 6 months after intra-amniotic injection of Ad.mTmG at E16 (Fig. 3A). The percentage of gene-edited $EGFP^{+}$ lung epithelial cells, the pulmonary cell lineage with highest gene editing efficiency, did not change over time, although there was a slight decrease in the number of gene-edited mesenchymal cells at later time points (Fig. 3B). We also assessed whether there were epithelial lineage–specific changes in the persistence of gene editing in the lung. The percentage of gene-edited secretory airway epithelial cells and ciliated airway epithelial cells remained stable over time, with only AT1 and AT2 cells demonstrating a slight decrease at P30 and 6 months, respectively (Fig. 3C). Thus, stable and highly specific gene editing is observed in most lung epithelial cells using the $R26^{mTmG/+}$ model (Fig. 3D).

Prenatal gene editing in $Sftpc^{I73T}$ mice decreases mutant SP-C^{I73T} proprotein and improves lung alveolarization

Because our data demonstrated effective and persistent gene editing in the developing lung, we next tested whether prenatal gene editing can rescue a clinically relevant monogenic human lung disease model. Among *SFTPC* variants associated with clinical ILD, the missense substitution (g.1286T > C), resulting in a change of isoleucine to threonine at position 73 in the SP-C proprotein ("SP-C^{I73T}"), is the most common known *SFTPC* mutation in humans (*7*, *37*). Functionally, expression of $SFTPC^{I73T}$ in vitro results in a toxic cellular response initiated by the markedly altered intracellular trafficking of the SP-C^{I73T} proprotein to the plasma membrane (*38*, *39*). The $Sftpc^{I73T}$ knockin mouse, which models human $SFTPC^{I73T}$, has shown that intracellular accumulation of mutant proprotein triggers an aberrant injury-repair response resulting in fibrotic lung remodeling in adult mice (*35*). Under appropriate conditions, $Sftpc^{I73T}$ mice can be induced to show an allele-dependent arrest of lung morphogenesis in late sacculation with no live births. Because previous studies have shown that *Sftpc* null mice have normal growth and lung function in homeostasis (*40*), we hypothesized that excision of the $Sftpc^{I73T}$ gene would reduce the synthesis of mistrafficked SP-C^{I73T} proprotein, thereby correcting the dysfunctional AT2 cell phenotype and improving survival in gene-edited $Sftpc^{I73T}$ mice (Fig. 4A).

sgRNAs were designed to target the 5′ and 3′ ends of the *Sftpc* gene and screened for efficient DNA cutting (fig. S4, A to D, and tables S1 and S2). Two Ad vectors containing SpyCas9 and EGFP cassette along with two of the selected sgRNAs (sgRNA 1A and 5B) for the *Sftpc* gene were used for intra-amniotic injections at E16 (collectively called the Ad.Sftpc.GFP). As predicted from the $R26^{mTmG/+}$ model, injected wild-type C57BL/6 fetuses demonstrated EGFP fluorescence in the lungs (Fig. 4, B and C) with $EGFP^{+}$ cells lining the lung epithelium (Fig. 4D). As expected, a large proportion of $CD45^{-}$/$DAPI^{-}$/$EPCAM^{+}$ cells were $EGFP^{+}$ on flow cytometry analysis, supporting efficient transduction of pulmonary epithelial cells using Ad.Sftpc.GFP (Fig. 4E). To determine whether CRISPR-mediated *Sftpc* excision and NHEJ occurred in fetal recipients of Ad.Sftpc.GFP, lung genomic DNA was assessed by PCR using primers flanking the *Sftpc* gene (table S3). The 605-bp band, corresponding to the excision of the *Sftpc* gene, was only present in fetuses that were $EGFP^{+}$ and was faint or absent in the fetuses that were $EGFP^{-}$ (fig. S4E). Sanger sequencing confirmed editing and NHEJ at the expected sites (fig. S4F). Analysis of FACS-sorted pulmonary epithelial cells from $EGFP^{+}$ lungs also confirmed deletion of the *Sftpc* gene and NHEJ at the expected sites (Fig. 4F). Last, to assess whether pulmonary cell transduction and editing could be improved by altering the timing of intra-amniotic injection, fetuses were injected with Ad.Sftpc.GFP at E14 or E17, and results were compared to those injected at E16 (fig. S4G). At all time points, intra-amniotic delivery of Ad.Sftpc.GFP resulted in gene editing in the lung (fig. S4, H and I, and table S4). Given the desire to maximize both the editing efficiency and time between editing and birth, we elected to use the E16 time point for rescue experiments in the $Sftpc^{I73T}$ mouse model.

The founder $Sftpc^{I73T\text{-}Neo}$ mouse line has a targeted allele containing an HA-tagged mouse $Sftpc^{I73T}$ sequence knocked into the endogenous mouse *Sftpc* locus (*35*). This allele contains an intronic flippase recognition target (FRT)–flanked phosphoglucokinase promoter (PGK)/neo cassette producing a milder phenotype. Deletion of the neo cassette using a homozygous FlpO deleter line results in increased expression of $Sftpc^{I73T}$ and a more severe phenotype characterized by abnormalities in sacculation, prenatal arrest of lung development, and perinatal death (fig. S4J). E16 $Sftpc^{I73T/WT}$ fetuses were injected with Ad.Null.GFP or Ad.Sftpc.GFP and harvested at E19 for analysis (Fig. 4G). $EGFP^{+}$ lungs were examined for *Sftpc* gene editing by PCR analysis using primers flanking the sgRNA target sites. The smaller 605-bp *Sftpc* gene-edited band was detected in the Ad.Sftpc.GFP-injected mice but not in the control Ad.Null.GFP-injected mice (fig. S4K). To quantify *Sftpc* gene editing, $EGFP^{+}$ lungs were examined by IHC for coexpression of SFTPB, an AT2 cell marker, and the HA tag, which should be deleted after CRISPR-mediated excision of the mutant allele. Whereas all the AT2 cells were HA^{+} in Ad.Null.GFP-injected fetuses, only 36% of the AT2 cells were HA^{+} in Ad.Sftpc.GFP-injected fetuses (Fig. 4, H and I). Ad.Null.GFP-injected fetuses demonstrated clusters of HA^{+} AT2 cells within compressed and poorly formed saccules of the $Sftpc^{I73T}$ mutant lungs, whereas Ad.Sftpc.GFP-injected lungs exhibited a greater number of normal-appearing saccules with AT2 cells showing a more typical punctate type of SFTPB staining, suggesting improved AT2 cell function. Furthermore, Ad.Sftpc.GFP-injected lungs also showed improved AT1 cell morphology as depicted by improved internuclear distance of HOPX-stained cells, signifying the characteristic cell spreading of AT1 cells (Fig. 4, J and K). To assess improvement in lung alveolarization after rescue, lungs of E19 fetuses were inflation-fixed for morphometric analysis. Ad.Sftpc.GFP-treated mice demonstrated decreased mean linear intercept (MLI) compared to Ad.Null.GFP-treated fetuses, indicating improved lung

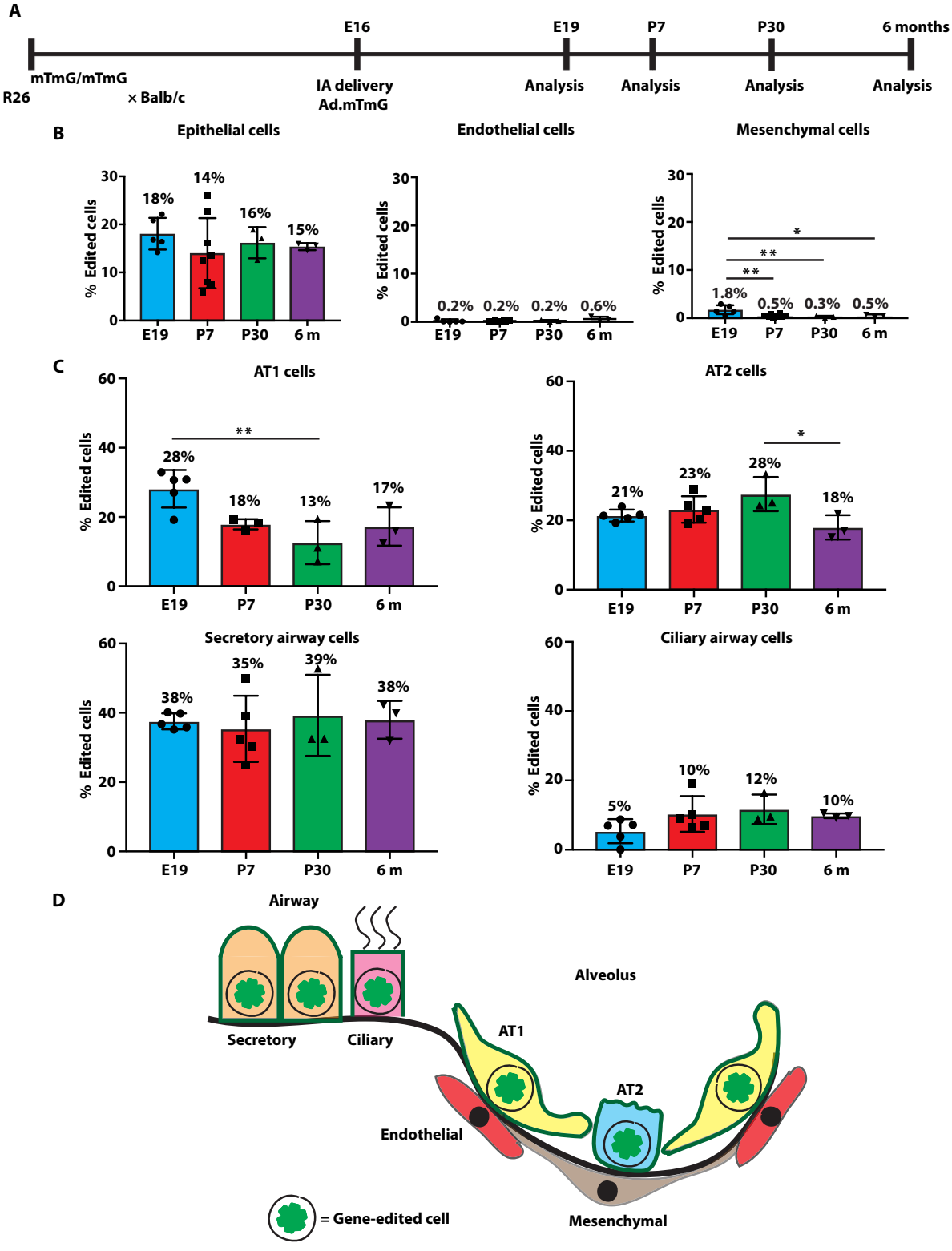

Fig. 3. Pulmonary epithelial cell gene editing is stable over time. (**A**) Experimental design for longer-term analysis of pulmonary epithelial cell gene editing after intra-amniotic Ad.mTmG delivery at E16. (**B**) Quantification of edited pulmonary epithelial, endothelial, and mesenchymal cell types at E19, P7, P30, and 6 months by FACS analysis. (**C**) Quantification of gene editing in individual pulmonary cell types at E19, P7, P30, and 6 months by IHC. (**D**) Schematic summary of fetal pulmonary cells that underwent gene editing after intra-amniotic delivery of CRISPR-Cas9 targeting the mT gene. $n = 3$ to 5 per group; $^{**}P < 0.01$ and $^{*}P < 0.05$ by one-way analysis of variance (ANOVA) followed by Tukey's multiple comparison test.

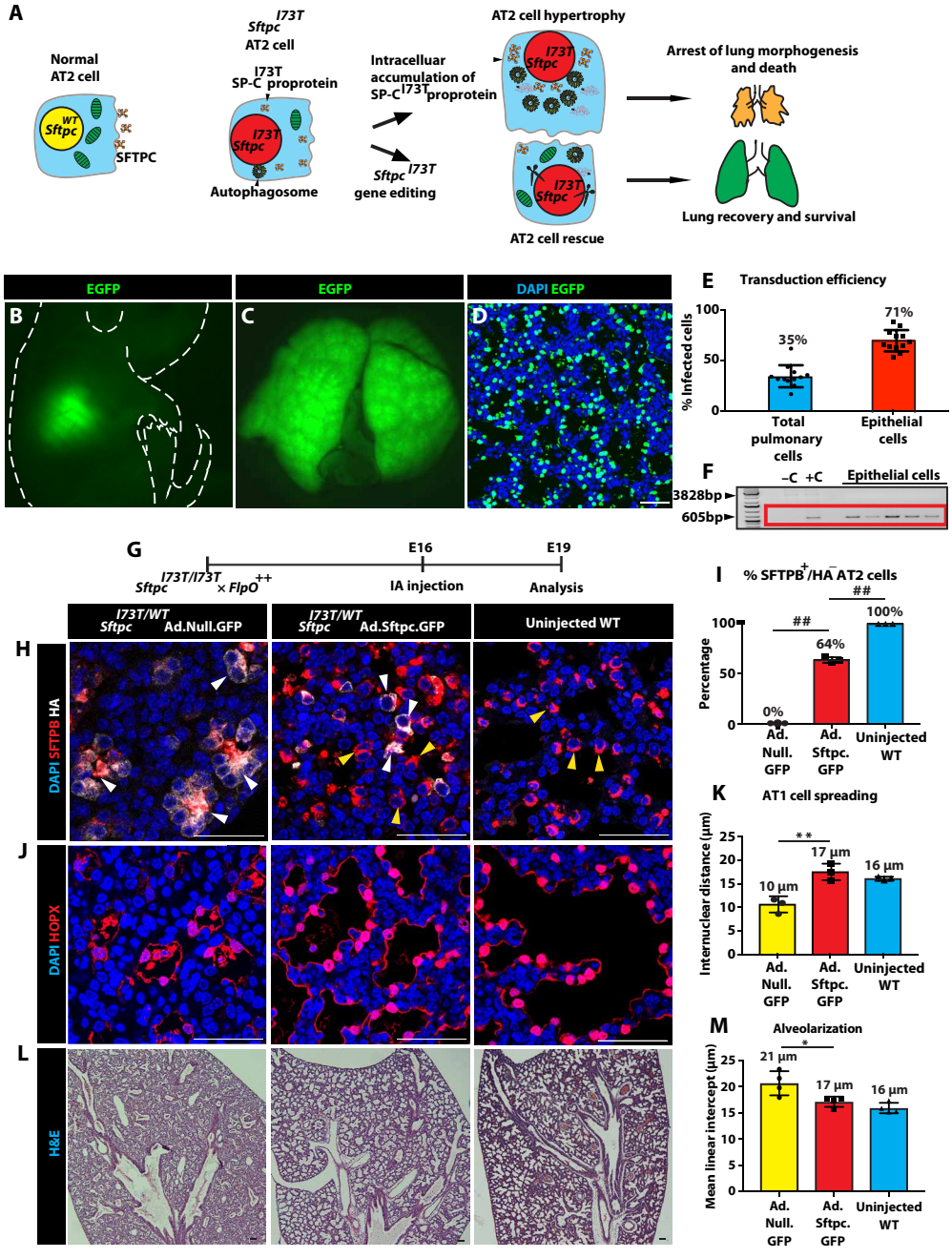

Fig. 4. Prenatal gene editing in *Sftpc*^{I73T} mice decreases mutant SP-C^{I73T} proprotein and improves lung alveolarization. (**A**) Schematic representation of *Sftpc*^{I73T} mutation causing intracellular accumulation of SP-C^{I73T} proprotein resulting in AT2 cell injury and potential cell rescue with CRISPR-Cas9–mediated excision of *Sftpc*^{I73T}. (**B**) Fluorescent stereomicroscopy, using a filter to detect EGFP, of an E19 fetus (outlined by white dashed line) after intra-amniotic injection of Ad.Sftpc.GFP at E16 shows green fluorescence in the chest region. (**C**) Fluorescent stereomicroscopy, using a filter to detect EGFP, of lungs at E19 after E16 intra-amniotic injection of Ad.Sftpc.GFP. (**D**) IHC for EGFP of lung parenchyma at E19 after E16 intra-amniotic injection of Ad.Sftpc.GFP. (**E**) FACS analysis to assess EGFP expression in all pulmonary cells and pulmonary epithelial cells (EPCAM$^+$ cells) from E19 fetuses after E16 intra-amniotic injection of Ad.Sftpc.GFP. $n = 10$ to 11 per group. (**F**) PCR analysis of DNA from E19 lung epithelial cells (EPCAM$^+$-sorted cells) of E16 Ad.Sftpc.GFP intra-amniotic injected fetuses. Edited *Sftpc* band, 605 bp; –C and +C, negative and positive controls consisting of nontransfected mouse neuro-2a cells and mouse N2a cells cotransfected with plasmids containing spyCas9 or sgRNA1-A and sgRNA5-B, respectively. (**G**) Schematic of *Sftpc*^{I73T} experimental design. (**H**) Excision of the mutant *Sftpc* allele in AT2 cells was assessed by IHC. Lungs of E19 *Sftpc*$^{I73T/WT}$ mice were assessed for expression of surfactant protein B (SFTPB) and hemagglutinin (HA) after E16 intra-amniotic injection of Ad.Null.GFP or Ad.Sftpc.GFP. SFTPB$^+$HA$^–$ (yellow arrowheads indicate representative cells), excision; SFTPB$^+$HA$^+$ (white arrowheads indicate representative cells), no excision; control, uninjected WT E19 lungs. (**I**) The percentage of SFTPB$^+$HA$^–$ cells on IHC was quantified. (**J**) Lung IHC for homeodomain only protein X (HOPX) at E19 to assess AT1 cell morphology and spreading in *Sftpc*$^{I73T/WT}$ mice injected with Ad.Null.GFP or Ad.Sftpc.GFP at E16. (**K**) The internuclear distance was measured to quantify AT1 spreading. (**L**) Hematoxylin and eosin (H&E) staining of lungs from E19 *Sftpc*$^{I73T/WT}$ mice injected at E16 with Ad.Null.GFP or Ad.Sftpc.GFP to assess alveolarization and sacculation. (**M**) The MLI was calculated to assess alveolarization. $n = 3$ to 4 per group; $^{\#\#}P < 0.0001$, $^{**}P < 0.01$, and $^{*}P < 0.05$ by one-way ANOVA followed by Tukey's multiple comparison test. WT, wild-type. Scale bars, 50 µm.

sacculation (Fig. 4, L and M). Further analysis by transmission electron microscopy revealed the presence of more mature AT2 cells with lamellar bodies and release of surfactant vesicles into the airspace lumen in Ad.Sftpc.GFP-injected mice, whereas the Ad.Null.GFP-injected mice showed tufts of hypertrophied AT2 cells with excessive autophagosomes and immature lamellar bodies (fig. S5). Next-generation sequencing (NGS) analysis of indels from 20 top off-target sites as predicted by CRISPOR (*41*) in lung genomic DNA from Ad.Sftpc.GFP-injected and uninjected *Sftpc*$^{I73T/WT}$ fetuses showed that indel rates in experimental animals were equal to those seen in the control for all sites (tables S5 and S6).

Prenatal gene editing in *Sftpc*^{I73T} mutant mice improves survival

Because CRISPR-mediated excision of the *Sftpc*^{I73T} gene decreased the synthesis of the mutant SP-C^{I73T} proprotein, improved AT2 and AT1 cell morphology and function, and improved lung maturation, we next tested whether gene-edited mice exhibited improved survival. E16 *Sftpc*$^{I73T/WT}$ fetuses were injected intra-amniotically with Ad.Null.GFP or Ad.Sftpc.GFP and assessed for survival up to 1 week of age (Fig. 5A). At baseline, this technique resulted in about 25% survival of C57BL/6 mice injected with Ad.Sftpc.GFP (n = 9 of 36). Whereas none of the *Sftpc*$^{I73T/WT}$ fetuses injected with the control Ad.Null.GFP construct (n = 0 of 36) survived beyond 6 hours after birth, a sizeable percentage of *Sftpc*$^{I73T/WT}$ fetuses injected with Ad.Sftpc.GFP (n = 7 of 87) survived beyond 24 hours (8%), including 5.7% (5 of 87) surviving to P7 (P = 0.005), at which point they remained healthy as indicated by normal activity, respiratory effort, subjective growth, and the presence of a milk spot (visualized from P0 to P2) indicative of feeding (Fig. 5B and movie S2). Surviving animals were sacrificed at P7 to assess pulmonary histology. Using the C57BL/6 Ad.Sftpc.GFP-treated fetuses as a baseline, these data demonstrate a 22.8% improvement in survival of *Sftpc*^{I73T} mutant Ad.Sftpc.GFP-treated fetuses (Fig. 5C). In the surviving cohort, there was a marked improvement in lung alveolarization at P7, with comparable MLI between *Sftpc*$^{I73T/WT}$ and C57BL/6 mice injected with Ad.Sftpc.GFP (Fig. 5, D and E). Sixty-eight percent of AT2 cells marked by SFTPB were HA$^-$, which is similar to that demonstrated at E19 (Fig. 5, F and G), and AT1 cell spreading was comparable to that seen in C57BL/6 fetuses injected with Ad.Sftpc.GFP (Fig. 5, H and I). Furthermore, a limited number of rescued animals were analyzed at 13 weeks (fig. S6A). MLI of Ad.Sftpc.GFP-injected *Sftpc*$^{I73T/WT}$ mice was comparable to that of Ad.Sftpc.GFP-injected C57BL/6 mice at this time point (fig. S6, B and C). Ninety-five percent of SFTPB$^+$ AT2 cells were HA$^-$ in Ad.Sftpc.GFP-injected *Sftpc*$^{I73T/WT}$ mice, and the morphology of AT1 cells was comparable between Ad.Sftpc.GFP-injected *Sftpc*$^{I73T/WT}$ and C57BL/6 mice (fig. S6, D to G). Our data demonstrate that fetal lung gene editing is feasible after intra-amniotic delivery of CRISPR-Cas9 and has the potential to attenuate embryonic toxic gain-of-function SP disease.

DISCUSSION

In this study, we demonstrate that CRISPR-Cas9 can be used to perform gene editing during tissue development through in utero intra-amniotic delivery to rescue a perinatal lethal monogenic lung disease. This approach targets the lung, with pulmonary epithelial cells including AT1, AT2, and secretory airway epithelial cells being preferentially edited. We show that in utero gene editing can ameliorate the phenotype of a congenital lung disease caused by the *Sftpc*^{I73T} mutation and improves survival of rescued mice. This proof-of-concept study supports an important application of CRISPR-Cas9 to rescue viability at birth due to a lethal genetic mutation.

The design of the *R26*$^{mTmG/+}$ model allowed for the tracking of cell type specificity, efficiency, and long-term persistence of gene editing. Our results demonstrate gene editing occurring predominantly in the lung and persisting up to 6 months of life, the last point of analysis. Using the intra-amniotic route of delivery, we were able to achieve about 20% editing in the lung epithelium, including the distally located AT1 and AT2 cells, at birth. Increased pulmonary epithelial cell editing compared to pulmonary endothelial and mesenchymal cell editing is likely due to direct contact between epithelial cells and the "inhaled" amniotic fluid and the location of Ad receptors on pulmonary epithelial cells that facilitate transduction (*33*, *42*, *43*).

In addition to pulmonary cell editing, we identified a few clusters of gene-edited cells in the proximal gastrointestinal tract after "swallowing" the amniotic fluid containing the viral vector, as previously demonstrated (*33*). Lower gastric compared to pulmonary cell editing might be due to the fairly rapid amniotic fluid inhalation, which was promoted by the administration of theophylline and maternal hypercarbia to enhance fetal breathing movements. Intra-amniotic injection might also be expected to target the skin. The lack of skin gene editing is likely explained by the skin barrier, formed initially by the periderm at E13 and completed by E17 after keratinization, which prevents viral vector transduction and thus epidermal editing after intra-amniotic delivery at E16 (*31*, *33*). Lung-targeted gene editing is an advantage for genes that specifically cause lung disease, although they may be expressed in other organs. Thus, a targeted approach may minimize the exposure of other organs to potentially deleterious on- and off-target effects. Although lung-specific gene editing is beneficial for SP disease in the current study, alternative delivery approaches, including the intravenous route, may allow for efficient prenatal editing of other organs to address congenital genetic disorders that cause morbidity and mortality before or shortly after birth (*27*). Last, although the use of theophylline and CO_2 to increase respiratory drive favored lung targeting in fetal mice via the intra-amniotic route, a more directed fetoscopic intratracheal approach could be performed in large animal models and in humans (*44*, *45*).

Another advantage of in utero gene editing is the relatively uniform targeting of most of the major pulmonary epithelial cell types, including both proximal and distal lineages. In general, the inhalational route of drug delivery to postnatal lungs results in a differential distribution, with peripheral regions of the lungs receiving lower amounts compared to proximal and central regions (*46*). The efficiency of inhalational drug distribution is further impaired in the injured lung because of heterogeneity of lung disease, with some regions of the lung being overinflated and other regions collapsed. Thus, particularly for more complex lung disease, the more uniform distribution of vector delivery observed via an in utero intervention may provide an advantage in future therapies.

Given that many congenital lung diseases such as cystic fibrosis and inherited SP disease are generally caused by monogenic mutations, they should be ideal candidates for gene editing technologies. In mice, *Sftpc* expression is not required for survival and lung function at normal physiologic conditions (*40*), and thus, a simple deletion

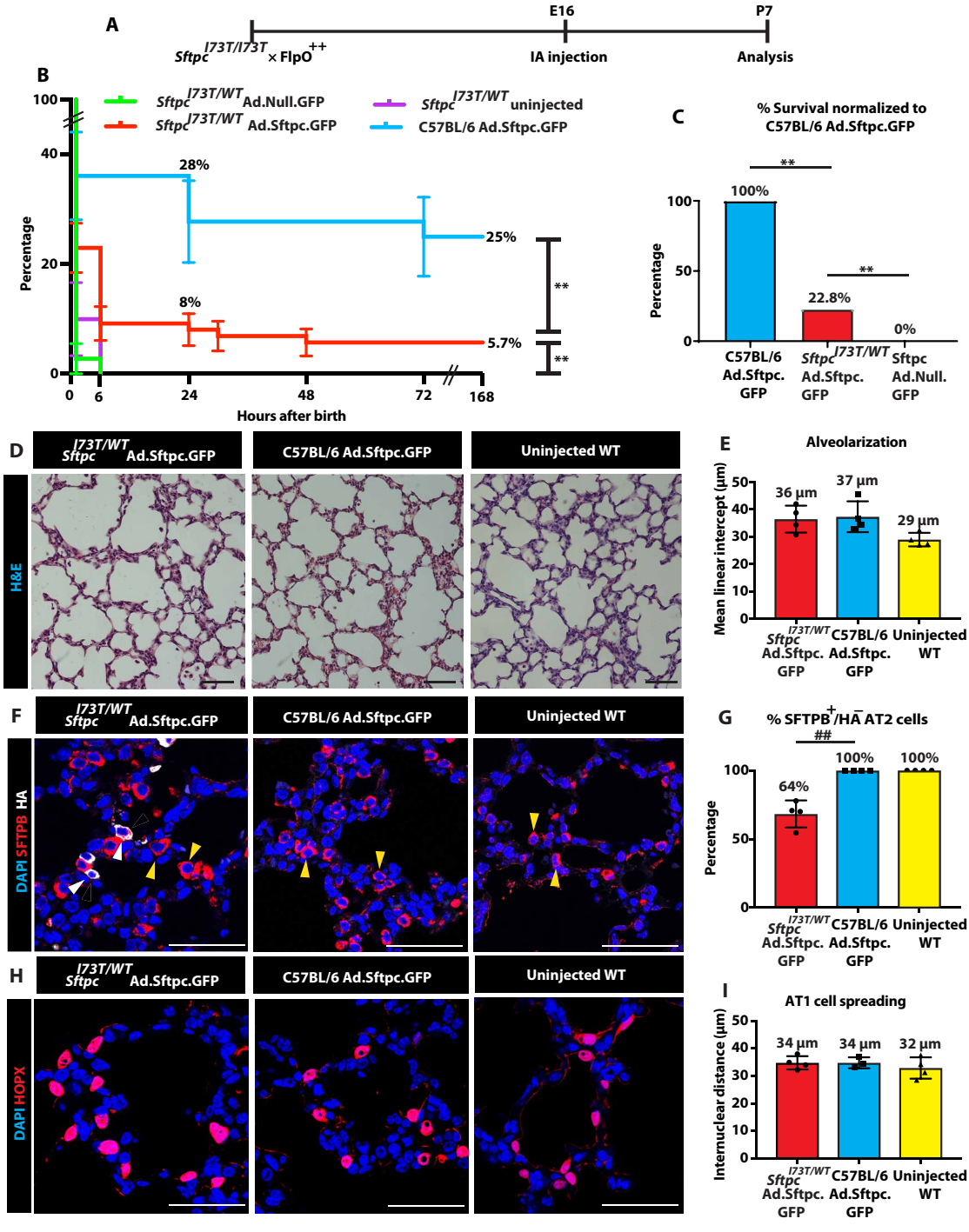

Fig. 5. Prenatal gene editing in *Sftpc*^{I73T} mutant mice improves survival. (**A**) Schematic of experimental design for survival analysis of *Sftpc*^{I73T} mutant mice. (**B**) Survival of C57BL/6 mice injected at E16 with Ad.Sftpc.GFP (blue), gene-edited *Sftpc*$^{I73T/WT}$ mice injected with Ad.Sftpc.GFP at E16 (red), *Sftpc*$^{I73T/WT}$ mice injected with Ad.Null.GFP at E16 (green), and uninjected *Sftpc*$^{I73T/WT}$ mice (purple). (**C**) The survival frequency of Ad.Sftpc.GFP-treated *Sftpc*$^{I73T/WT}$ mice was normalized to the survival rate of control C57BL/6-treated mice at 1 week of age. $n = 20$ to 87 per group; $^{**}P < 0.01$ by log-rank (Mantel-Cox) test for comparison of survival curves. (**D**) H&E staining of lungs from 1-week-old *Sftpc*$^{I73T/WT}$ mice and C57BL/6 mice injected with Ad.Sftpc.GFP at E16 and uninjected WT C57BL/6 mice was performed to assess alveolarization. (**E**) The MLI was calculated to assess alveolarization. (**F**) IHC for SFTPB and HA was performed on lungs from 1-week-old *Sftpc*$^{I73T/WT}$ mice and C57BL/6 mice injected with Ad.Sftpc.GFP at E16 and uninjected WT C57BL/6 mice to assess AT2 cell morphology and excision of the mutant *Sftpc* allele in AT2 cells. SFTPB$^+$HA$^-$ (yellow arrowheads indicate representative cells), excision; SFTPB$^+$HA$^+$ (white arrowheads indicate representative cells), no excision. (**G**) The percentage of SFTPB$^+$HA$^-$ cells, indicative of gene-edited cells in Ad.Sftpc.GFP injected *Sftpc*$^{I73T/WT}$ mice, was quantified on IHC. (**H**) IHC for HOPX was performed to assess AT1 cell morphology in 1-week-old *Sftpc*$^{I73T/WT}$ mice and C57BL/6 mice injected with Ad.Sftpc.GFP at E16 and uninjected WT C57BL/6 mice. (**I**) The internuclear distance was calculated to assess AT1 cell spreading. $n = 3$ to 4 per group; $^{\#\#}P < 0.0001$ by one-way ANOVA followed by Tukey's multiple comparison test. Scale bars, 50 µm.

of the mutant *Sftpc*^{I73T} gene was sufficient to improve mortality in our mouse model. Future therapeutic approaches in patients will likely require more targeted modifications in DNA. In humans, correction of the *SFTPC*^{I73T} mutation would be more desirable than excision of the mutated gene for treating the disease. However, our study demonstrates an important proof of concept regarding the feasibility of targeting the lung for gene editing before birth and presents evidence that even lethal mutations can be mitigated through prenatal gene editing techniques.

Limitations of our study include a high mortality rate at baseline after intra-amniotic viral vector delivery, the use of Ad as a delivery vehicle for CRISPR-Cas9, and the lack of robust long-term data including pulmonary function data in *Sftpc*^{I73T} mice prenatally treated with Ad.Sftpc.GFP. Although intra-amniotic viral vector injection into fetal mice has a high mortality, this is partly due to their small size, and this particular technical limitation would not be an issue in larger animals, including humans. However, the safety and efficacy of in utero gene editing in humans remain unknown, highlighting the importance of continued studies in small and large animal models, as well as humanized systems. We used Ad virus in the current study given its large packaging capacity and the size of SpyCas9, which is the most commonly used and most efficient Cas9 reported, and to ensure efficient transduction of pulmonary cells. However, adverse host immune responses are a known limitation to the clinical use of Ad vectors (*47*). Future studies using more clinically relevant delivery techniques, including adeno-associated viruses (AAVs) and/or lipid nanoparticles and smaller Cas9 genes, are required (*18*, *48*, *49*). Last, although we demonstrated improved survival and lung morphology at 1 week of age in *Sftpc*^{I73T} mice prenatally treated with Ad.Sftpc.GFP, demonstration of continued lung morphologic correction into adulthood correlating with improved pulmonary function in a larger cohort of mice is required.

Although prenatal gene editing has the potential to take advantage of normal developmental properties to enhance editing efficiency and treat perinatal lethal diseases before birth, additional points that are not present for postnatal gene editing must be considered. Any prenatal intervention involves the possibility of affecting not only the fetus but also the mother who is an immunocompetent and often disease-free "bystander." Thus, injection techniques and gene editing delivery vehicles will need to be optimized to avoid exposure to the mother. Given the potential maternal risk and only after rigorous animal studies demonstrate the safety and efficacy of prenatal gene editing, initial disease targets should include those that cause major morbidity and/or mortality before or shortly after birth and for which no adequate treatments exist. Prenatal gene editing could involve mid- to late-gestation gene editing as detailed in the current study or early embryo gene editing. Early embryo gene editing can be performed ex vivo, followed by implantation into the mother, thus avoiding maternal exposure to gene editing technology. In addition, early embryo gene editing may allow for more efficient correction of a larger number of cells in multiple organs, with the possibility of correcting germline cells. However, later-gestation gene editing may allow editing to be more specific for a target organ or cell population, including avoiding germ cell editing, and would allow for the possibility of treating de novo mutations diagnosed later in pregnancy.

With the rapid pace at which CRISPR technology is advancing toward clinical translation, techniques that improve the efficiency and specificity of gene editing for targeting specific organs or tissues associated with specific diseases are urgently needed. Our proof-of-concept studies demonstrating the feasibility of prenatal gene editing with high specificity for the lung represent a promising approach to address the unmet need for therapeutic approaches to congenital lung diseases that are fatal at birth.

MATERIALS AND METHODS

Study design

The objectives of this study were to evaluate, in mouse models, the feasibility and efficiency of prenatal lung gene editing after intra-amniotic delivery of CRISPR-Cas9 via Ad vector and to demonstrate that prenatal pulmonary gene editing can alter the phenotype of a perinatal lethal monogenic lung disease. Experimental animals were fetuses injected with viral vectors containing SpyCas9 and an sgRNA. Control animals were fetuses injected with viral vectors containing SpyCas9 and no sgRNA, Cre recombinase, or noninjected fetuses. Sample size was determined by availability and previous experience with in utero gene and cellular therapy experiments in the mouse model. No outliers were excluded from the study. A minimum of three animals per group were used for studies involving statistical analyses, and the *n* for individual experiments is indicated in the figure legends. Pregnant mice were randomly allocated to experimental and control groups. Intra-amniotic injections and dissections were conducted in a nonblinded fashion. Blinding was performed during data collection and analysis. when possible, given the survival and morphology differences in treated and untreated groups. For each experiment, sample size reflects the number of independent biological replicates.

Selection of sgRNAs

sgRNAs for the *R26*$^{mTmG/+}$ and *Sftpc*^{I73T} mouse models were chosen on the basis of high on-target efficiency and low off-target effects using the online tool at http://crispr.mit.edu (*12*). For *R26*$^{mTmG/+}$ mouse experiments, sgRNAs were designed to target both the loxP sites flanking the mT-tdTomato and stop cassette, causing the edited cells to express EGFP. For *Sftpc*^{I73T} mouse experiments, sgRNAs were designed to target the 5′ and 3′ ends of the *Sftpc* gene. The sgRNAs targeting the *Sftpc* gene were screened by Surveyor assay in vitro. Briefly, the *Sftpc* sgRNAs were cloned into plasmid pSpyCas9-(BB)-2A-GFP (PX458; a gift from F. Zhang; Addgene plasmid no. 48138) (*12*), which was used to transfect mouse neuro-2a cells. Genomic DNA was extracted using DNeasy blood and tissue kit (QIAGEN) 48 hours after transfection. Indel efficiency of each sgRNA was assessed by Surveyor nuclease assay (Integrated DNA Technologies) as previously described after amplifying with primers flanking the target site (*12*). The protospacer and PAM sequences screened and the PCR primers used in the Surveyor assay are listed in tables S1 and S2, respectively.

Generation of Ad vectors

The mTmG sgRNA was cloned into plasmid pX330-U6-Chimeric_BB-CBh-hSpyCas9 (a gift from F. Zhang; Addgene plasmid no. 42230) (*50*). The *Sftpc* sgRNAs (1A-targeting exon 1 and 5B-targeting exon 5), which were noted to have activity on Surveyor assay during in vitro screening, were used for the in vivo experiments. The plasmids *pX330*-U6-Chimeric_BB-CBh-hSpyCas9 and pSpyCas9(BB)-2A-GFP (PX458) in which no sgRNA was cloned served as the negative control for the *R26*$^{mTmG/+}$ and *Sftpc*^{I73T} mouse experiments, respectively.

Vector Biolabs used these constructs to generate recombinant Ad type 5 particles. Premade Ad type 5 particles containing Cre recombinase under a cytomegalovirus promoter were purchased from Penn Vector Core. Ad vectors are referred to as Ad.mTmG, Ad.Sftpc.GFP, Ad.Cre, Ad.Null, and Ad.Null.GFP. The final viral titer used for experiments ranged from 0.6×10^{10} to 1.2×10^{11} plaque-forming units/ml.

Animals

C57Bl/6, B6.129(Cg)-Gt(ROSA)26Sor$^{tm4(ACTB-tdTomato,-EGFP)Luo}$/J (called *R26*$^{mTmG/+}$; stock no. 007676), and B6.129S4-Gt(ROSA)26Sortm2(FLP*)Sor/J (called Flp-O mice; stock no. 12930) were purchased from the Jackson Laboratories. *Sftpc*^{I73T} mice were created and provided by M.F.B. (*35*). Animals were housed in the Laboratory Animal Facility of the Abramson Research Center and the Colket Translational Research Building at the Children's Hospital of Philadelphia (CHOP). The experimental protocols were approved by the Institutional Animal Care and Use Committee at the CHOP, and guidelines set forth in the National Institutes of Health's Guide for the Care and Use of Laboratory Animals were followed.

In utero injection

Intra-amniotic in utero injections were performed as previously described (movie S1) (*32*). Briefly, the amniotic cavity of fetuses of time-dated mice was injected at E16, a time during murine fetal development at which fetal breathing movements are optimal. Under isoflurane anesthesia and after providing local anesthetic (0.25% bupivacaine subcutaneously), a midline laparotomy was made, and the uterine horn was exposed. Under a dissecting microscope, 10 μl of virus combined with 10 μl of theophylline (1.6 mg/ml) were injected into the amniotic sac of each fetus. The uterus was then returned to the abdominal cavity, and the laparotomy incision was closed in a single layer with 4-0 Vicryl suture. After recovery from anesthesia, pregnant dams were placed in a chamber containing 10% CO_2 for 1 hour. Theophylline injection and maternal CO_2 exposure were performed to enhance fetal respiratory drive to more efficiently target the fetal lung (*40*).

R26^{mTmG} CRISPR gene editing model

The Gt(ROSA)26Sor$^{tm4(ACTB-tdTomato,-EGFP)Luo}$ (R26$^{mTmG/+}$) mouse model is a fluorescent reporter mouse model that consists of an mT-tdTomato and a 3′ stop codon that is flanked by loxP sites. Downstream to the distal loxP site is the mG-EGFP. All cells at baseline express tdTomato. Expression of Cre recombinase causes deletion of the mT-tdTomato cDNA along with a transcriptional stop cassette and expression of the mG-EGFP (*34*). R26$^{mTmG/+}$ fetuses were injected intra-amniotically with Ad.mTmG, Ad.Cre, or Ad.Null at E16, and the injected fetuses were analyzed at E19, P7, P30, and 6 months of age. At the time of analysis, the lungs and other organs of injected mice were assessed for EGFP expression by fluorescent stereomicroscope (MZ16 FA; Leica). For larger mice at P30 to 6 months of age, the right lung was fixed in 2% paraformaldehyde for IHC analysis, and the left lung was used to extract genomic DNA with DNeasy blood and tissue kit (QIAGEN) and for FACS. At E19 and P7, the right lung was used for IHC, and the left lung was used to extract DNA from a single mouse. Both the right and left lungs from another mouse were used for FACS. For the experimental group, all fetuses from a single dam were injected with Ad.mTmG. Ad.Cre was injected at comparable titers to all fetuses from another dam as a positive control, and Ad.Null without an sgRNA was injected at comparable titers for negative control experiments.

Sftpc^{I73T} mutant mouse model

The *Sftpc*^{I73T} mouse line has targeted alleles containing an HA-tagged mouse SP-C^{I73T} sequence knocked into the endogenous mouse *Sftpc* locus. Heterozygous mutant mice accumulate mistrafficked mutant SP-C^{I73T} proprotein within AT2 cells, causing arrest of lung morphogenesis and death within 6 hours of birth. An intronic FRT-PGK-neo-FRT cassette results in a hypomorphous phenotype and enables mice to survive to adulthood (*35*). In this study, *Sftpc*$^{I73T/I73T/Neo+/+}$ mice were crossed with *FlpO*$^{+/+}$ mice to produce *Sftpc*$^{I73T/WT}$ fetuses. Two Ad type 5 vectors with one virus expressing spyCas9, an sgRNA targeting the 5′ end of the *Sftpc* gene, and EGFP and the other virus expressing spyCas9, an sgRNA targeting the 3′ end of the *Sftpc* gene, and EGFP were injected into E16 *Sftpc*$^{I73T/WT}$ or C57BL/6 fetuses. Fetuses were harvested at E19 for analysis as described above. For survival analysis of *Sftpc*$^{I73T/WT}$-injected fetuses, pups were allowed to be born and fostered with Balb/c dams until P7, at which time they were euthanized by decapitation for morphological and IHC analysis.

Gene editing assessed by PCR analysis

Primers 5′ and 3′ to the sgRNA target sites in the *mTmG-loxP* and *Sftpc* genes were used for PCR analysis to detect gene editing (table S3). PCR amplification with mTmG primers results in a 2951-bp band for the unedited mTmG sequence and a 545-bp band for the edited mTmG sequence. Similarly, PCR amplification with *Sftpc* primers results in a 3828-bp band for the unedited *Sftpc*^{WT} gene, a 3950-bp band for the unedited *Sftpc*^{I73T} gene, and a 605-bp band for the edited *Sftpc* gene. For quantification of gene-edited *Sftpc* alleles, quantitative real-time PCR was performed on a QuantStudio 7 Flex using SYBR green reagents and primers specific for the unedited and edited alleles (table S4).

Lung cell isolation and flow cytometry

Lungs were harvested and processed into a single-cell suspension using a dispase (Collaborative Biosciences)/collagenase (Life Technologies)/DNase solution as previously described (*51*). For the *R26*^{mTmG} experiments, lung epithelial, endothelial, and mesenchymal cell populations were assessed using a MoFlo Astrios EQ (Beckman Coulter) flow cytometer with antibody staining for 4′,6-diamidino-2-phenylindole (DAPI), EPCAM-allophycocyanin (APC) (eBioscience), CD31-PECy7 (eBioscience), and CD45-ef450 (eBioscience). Cells were negatively gated for DAPI and CD45 channels to exclude dead cells and lymphohematopoietic cells. Pulmonary epithelial (EPCAM$^+$CD31$^-$), endothelial (EPCAM$^-$CD31$^+$), and mesenchymal (EPCAM$^-$CD31$^-$) cells were evaluated for EGFP expression to determine the percentage of editing within each cell type (fig. S2, E and F). Individual cell types were FACS-sorted, and DNA was extracted for PCR analysis as described above. Similarly, for the *Sftpc*^{I73T} mouse experiments, lung epithelial cell populations were sorted from the single-cell suspension using a MoFlo Astrios EQ (Beckman Coulter) flow cytometer with antibody staining for DAPI, EPCAM-APC (eBioscience), and CD45-PECy7 (eBioscience) and negatively gated for DAPI and CD45. The percentage of pulmonary epithelial cells transduced by Ad was measured by the percentage of EPCAM$^+$ cells that were EGFP$^+$. EPCAM$^+$ cells were sorted, and DNA was extracted for PCR analysis.

Histology and IHC

Lungs were directly fixed in 2% paraformaldehyde. Lungs that were harvested for morphological analyses were inflation-fixed with 20 cm of H_2O at E19 and 30 cm of H_2O at P7 or later. After serial dehydration, tissue was embedded in paraffin and sectioned. H&E staining was performed for tissue morphology. IHC to detect proteins was performed using the following antibodies on paraffin sections: GFP (goat, 1:100; Abcam), GFP (chicken, 1:500; Aves), red fluorescent protein (rabbit, 1:250; Rockland), SFTPC (rabbit, 1:250; Santa Cruz Biotechnology), SFTPB (rabbit, 1:500; Abcam), AQP5 (rabbit, 1:100; Abcam), SCGB1A1 (goat, 1:20; Santa Cruz Biotechnology), FOXJ1 (mouse, 1:250; Santa Cruz Biotechnology), HA (mouse, 1:4000; Abcam), and HOPX (mouse, 1:50; Santa Cruz Biotechnology).

Quantification of edited cells by IHC

Confocal microscopy using a Leica TCS SP8 confocal scope was used to capture images. For each mouse, confocal z-stack images were taken in 5 or 10 random airway and alveolar areas, respectively, and analyzed using ImageJ software. The specific cell types that were $EGFP^+$ in the $R26^{mTmG}$ experiments or HA^+ in $Sftpc^{I73T}$ experiments were manually counted using the Cell Counter plug-in for ImageJ.

Quantification of alveolarization and AT1 cell spreading

For quantification of MLI, 10 pictures for each sample were taken with a 40× objective lens for E19 lungs and at 20× for P7 and adult lungs. The images were viewed under a field of equally spaced horizontal lines using ImageJ, and MLI was calculated as the average of total length of lines divided by the total intercepts of alveolar septa from each lung. For quantification of AT1 cell spreading, five pictures from each lung sample were taken with a 40× objective, and average distance between HOPX-stained AT1 cells was measured using ImageJ as previously described (*52*).

Off-target analysis

Off-target sites for *Sftpc* were predicted using CRISPOR (http://crispor.tefor.net), and the top 20 sites, as ranked by the cutting frequency determination (CFD) off-target score (*41*), were assessed by next-generation DNA sequencing at the Massachusetts General Hospital Center for Computational and Integrative Biology DNA Core (CRISPR Sequencing Service; https://dnacore.mgh.harvard.edu/new-cgi-bin/site/pages/crispr_sequencing_main.jsp). Please refer to tables S5 and S6 for the predicted off-target sites and the PCR primers used for off-target NGS analysis. The number of paired-end reads typically exceeded 50,000 per target site per sample. Off-target indel mutagenesis rates were determined as previously described (*18*).

Statistical analyses

At least three mice were used for experimental and control groups undergoing statistical analyses, with the n values indicated in the figure legends. All animals that inhaled the virus after intra-amniotic delivery, as represented by $EGFP^+$ lungs, were included for the final analysis. Animals that had $EGFP^-$ lungs were considered as technical failure and excluded from final analysis. All data points used in statistical analyses are represented as the means ± 1 SD. For histologic analyses, all data points were means of technical replicates and presented as percentages or means ± 1 SD. A two-tailed Student's t test was used for experiments involving the comparison of two groups in which data were normally distributed, as determined by the Shapiro-Wilk test of normality. A one-way ANOVA followed by Tukey's multiple comparison tests was used for statistical analyses of experiments involving the comparison of more than two groups. Survival analysis of gene-edited $Sftpc^{I73T}$ mice was performed using survival proportions and by log-rank (Mantel-Cox) test for comparison of survival curves. $P < 0.05$ was considered significant. Statistical analyses were performed with GraphPad Prism 7. Original data are in data file S1.

SUPPLEMENTARY MATERIALS

stm.sciencemag.org/cgi/content/full/11/488/eaav8375/DC1

Fig. S1. $R26^{mTmG}$ gene locus of interest and lack of gene editing in nonpulmonary organs after intra-amniotic delivery.
Fig. S2. Distribution of gene-edited cells in the lung.
Fig. S3. Gene editing in pulmonary cell types.
Fig. S4. Selection of sgRNAs for excision of the *Sftpc* gene and in vivo gene editing in C57BL/6 and $Sftpc^{I73T/WT}$ mice.
Fig. S5. Transmission electron microscopy of gene-edited lungs of $Sftpc^{I73T/WT}$ mice.
Fig. S6. Lung morphology of gene-edited $Sftpc^{I73/WT}$ mice in adulthood.
Table S1. mTmg and *Sftpc* sgRNAs for in vitro and in vivo editing.
Table S2. Primers used for surveyor assay for *Sftpc* sgRNAs.
Table S3. Primers used for PCR and Sanger sequencing.
Table S4. Primers used for qPCR for *Sftpc* gene deletion.
Table S5. Primer sequences for NGS of *Sftpc* off-target sites.
Table S6. Analysis of 20 off-target sites.
Movie S1. Intra-amniotic injection of dilute trypan blue at E16.
Movie S2. In utero gene-edited $Sftpc^{I73T/WT}$ mouse at P7.
Data file S1. Original data.

REFERENCES AND NOTES

1. A. Hamvas, F. S. Cole, L. M. Nogee, Genetic disorders of surfactant proteins. *Neonatology* **91**, 311–317 (2007).
2. J. A. Whitsett, S. E. Wert, T. E. Weaver, Alveolar surfactant homeostasis and the pathogenesis of pulmonary disease. *Annu. Rev. Med.* **61**, 105–119 (2010).
3. S. M. Rowe, S. Miller, E. J. Sorscher, Cystic fibrosis. *N. Engl. J. Med.* **352**, 1992–2001 (2005).
4. R. G. Crystal, Alpha 1-antitrypsin deficiency, emphysema, and liver disease. Genetic basis and strategies for therapy. Genetic basis and strategies for therapy. *J. Clin. Invest.* **85**, 1343–1352 (1990).
5. K. A. Spoonhower, P. B. Davis, Epidemiology of cystic fibrosis. *Clin. Chest Med.* **37**, 1–8 (2016).
6. H. A. Tanash, P. M. Nilsson, J. A. Nilsson, E. Piitulainen, Clinical course and prognosis of never-smokers with severe alpha-1-antitrypsin deficiency (PiZZ). *Thorax* **63**, 1091–1095 (2008).
7. H. S. Cameron, M. Somaschini, P. Carrera, A. Hamvas, J. A. Whitsett, S. E. Wert, G. Deutsch, L. M. Nogee, A common mutation in the surfactant protein C gene associated with lung disease. *J. Pediatr.* **146**, 370–375 (2005).
8. L. M. Nogee, Interstitial lung disease in newborns. *Semin. Fetal Neonatal Med.* **22**, 227–233 (2017).
9. W. B. Eldridge, Q. Zhang, A. Faro, S. C. Sweet, P. Eghtesady, A. Hamvas, F. S. Cole, J. A. Wambach, Outcomes of lung transplantation for infants and children with genetic disorders of surfactant metabolism. *J. Pediatr.* **184**, 157–164.e2 (2017).
10. S. Kirkby, D. Hayes Jr., Pediatric lung transplantation: Indications and outcomes. *J. Thorac. Dis.* **6**, 1024–1031 (2014).
11. J. A. Doudna, E. Charpentier, Genome editing. The new frontier of genome engineering with CRISPR-Cas9. *Science* **346**, 1258096 (2014).
12. F. A. Ran, P. D. Hsu, J. Wright, V. Agarwala, D. A. Scott, F. Zhang, Genome engineering using the CRISPR-Cas9 system. *Nat. Protoc.* **8**, 2281–2308 (2013).
13. P. Mali, K. M. Esvelt, G. M. Church, Cas9 as a versatile tool for engineering biology. *Nat. Methods* **10**, 957–963 (2013).
14. H. Ma, N. Marti-Gutierrez, S. W. Park, J. wu, Y. Lee, K. Suzuki, A. Koski, D. Ji, T. Hayama, R. Ahmed, H. Darby, C. Van Dyken, Y. Li, E. Kang, A. R. Park, D. Kim, S. T. kim, J. Gong, Y. Gu, X. Xu, D. Bataglia, S. A. Krieg, D. M. Lee, D. H. Wu, D. P. Wolf, S. B. Heitner, J. C. I. Belmonte, P. Amato, J. S. Kim, S. Kaul, S. Mitalipov, Correction of a pathogenic gene mutation in human embryos. *Nature* **548**, 413–419 (2017).
15. S. Q. Tsai, J. K. Joung, Defining and improving the genome-wide specificities of CRISPR-Cas9 nucleases. *Nat. Rev. Genet.* **17**, 300–312 (2016).
16. C. E. Nelson, C. H. Hakim, D. G. Ousterout, P. I. Thakore, E. A. Moreb, R. M. Castellanos Rivera, S. Madhavan, X. Pan, F. A. Ran, W. X. Yan, A. Asokan, F. Zhang, D. Duad, C. A. Gersbach, In vivo genome editing improves muscle function in a mouse model of Duchenne muscular dystrophy. *Science* **351**, 403–407 (2016).
17. M. Tabebordbar, K. Zhu, J. K. Cheng, W. L. Chew, J. J. Widrick, W. X. Yan, C. Masener, E. Y. Wu, R. Xiao, F. A. Ran, L. Cong, F. Zhang, L. H. Vandenberghe, G. M. Church,

A. J. Wagers, In vivo gene editing in dystrophic mouse muscle and muscle stem cells. *Science* **351**, 407–411 (2016).
18. Y. Yang, L. Wang, P. Bell, D. McMenamin, Z. He, J. White, H. Yu, C. Xu, H. Morizono, K. Musunuru, M. L. Batshaw, J. M. Wilson, A dual AAV system enables the Cas9-mediated correction of a metabolic liver disease in newborn mice. *Nat. Biotechnol.* **34**, 334–338 (2016).
19. C. Q. Song, D. Wang, T. Jiang, K. O'Connor, Q. Tang, L. Cai, X. Li, Z. Weng, H. Yin, G. Gao, C. Mueller, T. R. Flotte, W. Xue, In vivo genome editing partially restores alpha-1 antitrypsin in a murine model of AAT deficiency. *Hum. Gene Ther.* **29**, 853–860 (2018).
20. Y. Wu, D. Liang, Y. Wang, M. Bai, W. Tang, S. Bao, Z. Yan, D. Li, J. Li, Correction of a genetic disease in mouse via use of CRISPR-Cas9. *Cell Stem Cell* **13**, 659–662 (2013).
21. M. El Refaey, L. Xu, Y. Gao, B. D. Canan, T. M. A. Adesanya, S. C. Warner, K. Akagi, D. E. Symer, P. J. Mohler, J. Ma, P. M. L. Janssen, R. Han, In vivo genome editing restores dystrophin expression and cardiac function in dystrophic mice. *Circ. Res.* **121**, 923–929 (2017).
22. N. M. E. Fogarty, A. McCarthy, K. E. Snijders, B. E. Powell, N. Kubikova, P. Blakeley, R. Lea, K. Elder, S. E. Wamaitha, D. Kim, V. Maciulyte, J. Kleinjung, J. S. Kim, D. Wells, L. Vallier, A. Bertero, J. M. A. Turner, K. K. Niakan, Genome editing reveals a role for OCT4 in human embryogenesis. *Nature* **550**, 67–73 (2017).
23. C. Long, J. R. McAnally, J. M. Shelton, A. A. Mireault, R. Bassel-Duby, E. N. Olson, Prevention of muscular dystrophy in mice by CRISPR/Cas9-mediated editing of germline DNA. *Science* **345**, 1184–1188 (2014).
24. J. Wu, M. Vilarino, K. Suzuki, D. Okamura, Y. S. Bogliotti, I. Park, J. Rowe, B. McNabb, P. J. Ross, J. C. I. Belmonte, CRISPR-Cas9 mediated one-step disabling of pancreatogenesis in pigs. *Sci. Rep.* **7**, 10487 (2017).
25. M. S. Carlon, D. Vidović, J. Dooley, M. M. da Cunha, M. Maris, Y. Lampi, J. Toelen, C. Van den Haute, V. Baekelandt, J. Deprest, E. Verbeken, A. Liston, R. Gijsbers, Z. Debyser, Immunological ignorance allows long-term gene expression after perinatal recombinant adeno-associated virus-mediated gene transfer to murine airways. *Hum. Gene Ther.* **25**, 517–528 (2014).
26. M. G. Davey, J. S. Riley, A. Andrews, A. Tyminski, M. Limberis, J. E. Pogoriler, E. Patridge, A. Olive, H. L. Hedrick, A. W. Flake, W. H. Peranteau, Induction of immune tolerance to foreign protein via adeno-associated viral vector gene transfer in mid-gestation fetal sheep. *PLOS ONE* **12**, e0171132 (2017).
27. A. C. Rossidis, J. D. Stratigis, A. C. Chadwick, H. A. Hartman, N. J. Ahn, H. Li, K. Singh, B. E. Coons, L. Li, W. Lv, P. W. Zoltick, D. Alapati, W. Zacharias, R. Jain, E. E. Morrisey, K. Musunuru, W. H. Peranteau, In utero CRISPR-mediated therapeutic editing of metabolic genes. *Nat. Med.* **24**, 1513–1518 (2018).
28. D. E. Sabatino, T. C. Mackenzie, W. Peranteau, S. Edmonson, C. Campagnoli, Y. L. Liu, A. W. Flake, K. A. High, Persistent expression of hF.IX after tolerance induction by in utero or neonatal administration of AAV-1-F.IX in hemophilia B mice. *Mol. Ther.* **15**, 1677–1685 (2007).
29. G. A. Duncan, J. Jung, J. Hanes, J. S. Suk, The mucus barrier to inhaled gene therapy. *Mol. Ther.* **24**, 2043–2053 (2016).
30. P. L. Sinn, E. R. Burnight, P. B. McCray Jr., Progress and prospects: Prospects of repeated pulmonary administration of viral vectors. *Gene Ther.* **16**, 1059–1065 (2009).
31. M. Endo, T. Henriques-Coelho, P. W. Zoltick, D. H. Stitelman, W. H. Peranteau, A. Radu, A. W. Flake, The developmental stage determines the distribution and duration of gene expression after early intra-amniotic gene transfer using lentiviral vectors. *Gene Ther.* **17**, 61–71 (2010).
32. L. Joyeux, E. Danzer, M. P. Limberis, P. W. Zoltick, A. Radu, A. W. Flake, M. G. Davey, In utero lung gene transfer using adeno-associated viral and lentiviral vectors in mice. *Hum. Gene Ther. Methods* **25**, 197–205 (2014).
33. S. M. Buckley, S. N. Waddington, S. Jezzard, L. Lawrence, H. Schneider, M. V. Holder, M. Themis, C. Coutelle, Factors influencing adenovirus-mediated airway transduction in fetal mice. *Mol. Ther.* **12**, 484–492 (2005).
34. M. D. Muzumdar, B. Tasic, K. Miyamichi, L. Li, L. Luo, A global double-fluorescent Cre reporter mouse. *Genesis* **45**, 593–605 (2007).
35. S. I. Nureki, Y. Tomer, A. Venosa, L. Katzen, S. J. Russo, S. Jamil, M. Barrett, V. Nguyen, M. Kopp, S. Mulugeta, M. F. Beers, Expression of mutant Sftpc in murine alveolar epithelia drives spontaneous lung fibrosis. *J. Clin. Invest.* **128**, 4008–4024 (2018).
36. M. Kosicki, K. Tomberg, A. Bradley, Repair of double-strand breaks induced by CRISPR-Cas9 leads to large deletions and complex rearrangements. *Nat. Biotechnol.* **36**, 765–771 (2018).
37. F. Brasch, M. Griese, M. Tredano, G. Johnen, M. Ochs, C. Rieger, S. Mulugeta, K. M. Muller, M. Bahuau, M. F. Beers, Interstitial lung disease in a baby with a de novo mutation in the SFTPC gene. *Eur. Respir. J.* **24**, 30–39 (2004).
38. M. F. Beers, A. Hawkins, J. A. Maguire, A. Kotorashvili, M. Zhao, J. L. Newitt, W. Ding, S. Russo, S. Guttentag, S. Gonzales, S. Mulugeta, A nonaggregating surfactant protein C mutant is misdirected to early endosomes and disrupts phospholipid recycling. *Traffic* **12**, 1196–1210 (2011).
39. A. Hawkins, S. Guttentag, R. Deterding, W. K. Funkhouser, J. L. Goralski, S. Chatterjee, S. Mulugeta, M. F. Beers, A non-BRICHOS SFTPC mutant (SP-CI73T) linked to interstitial lung disease promotes a late block in macroautophagy disrupting cellular proteostasis and mitophagy. *Am. J. Physiol. Lung Cell. Mol. Physiol.* **308**, L33–L47 (2015).
40. S. W. Glasser, M. S. Burhans, T. R. Korfhagen, C. L. Na, P. D. Sly, G. F. Ross, M. Ikegami, J. A. Whitsett, Altered stability of pulmonary surfactant in SP-C-deficient mice. *Proc. Natl. Acad. Sci. U.S.A.* **98**, 6366–6371 (2001).
41. M. Haeussler, K. Schönig, H. Eckert, A. Eschstruth, J. Mianné, J.-B. Renaud, S. Schneider-Maunoury, A. Shkumatava, L. Teboul, J. Kent, J.-S. Joly, J.-P. Concordet, Evaluation of off-target and on-target scoring algorithms and integration into the guide RNA selection tool CRISPOR. *Genome Biol.* **17**, 148 (2016).
42. N. Arnberg, Adenovirus receptors: Implications for targeting of viral vectors. *Trends Pharmacol. Sci.* **33**, 442–448 (2012).
43. A. L. Cooney, B. K. Singh, L. M. Loza, I. M. Thornell, C. E. Hippee, L. S. Powers, L. S. Ostedgaard, D. K. Meyerholz, C. Wohlford-Lenane, D. A. Stoltz, P. B. McCray Jr., P. L. Sinn, Widespread airway distribution and short-term phenotypic correction of cystic fibrosis pigs following aerosol delivery of piggyBac/adenovirus. *Nucleic Acids Res.* **46**, 9591–9600 (2018).
44. A. L. David, D. M. Peebles, L. Gregory, M. Themis, T. Cook, C. Coutelle, C. H. Rodeck, Percutaneous ultrasound-guided injection of the trachea in fetal sheep: A novel technique to target the fetal airways. *Fetal Diagn. Ther.* **18**, 385–390 (2003).
45. M. R. Harrison, R. L. Keller, S. B. Hawgood, J. A. Kitterman, P. L. Sandberg, D. L. Farmer, H. Lee, R. A. Filly, J. A. Farrell, C. T. Albanese, A randomized trial of fetal endoscopic tracheal occlusion for severe fetal congenital diaphragmatic hernia. *N. Engl. J. Med.* **349**, 1916–1924 (2003).
46. N. R. Labiris, M. B. Dolovich, Pulmonary drug delivery. Part I: Physiological factors affecting therapeutic effectiveness of aerosolized medications. *Br. J. Clin. Pharmacol.* **56**, 588–599 (2003).
47. Y. S. Ahi, D. S. Bangari, S. K. Mittal, Adenoviral vector immunity: Its implications and circumvention strategies. *Curr. Gene Ther.* **11**, 307–320 (2011).
48. E. Kim, T. Koo, S. W. Park, D. Kim, K. Kim, H. Y. Cho, D. W. Song, K. J. Lee, M. H. Jung, S. Kim, J. H. Kim, J. S. Kim, In vivo genome editing with a small Cas9 orthologue derived from campylobacter jejuni. *Nat. Commun.* **8**, 14500 (2017).
49. H. Yin, C. Q. Song, S. Suresh, Q. Wu, S. Walsh, L. H. Rhym, E. Mintzer, M. F. Bolukbasi, L. J. Zhu, K. Kauffman, H. Mou, A. Oberholzer, J. Ding, S. Y. Kwan, R. L. Bogorad, T. Zatsepin, V. Koteliansky, S. A. Wolfe, W. Xue, R. Langer, D. G. Anderson, Structure-guided chemical modification of guide RNA enables potent non-viral in vivo genome editing. *Nat. Biotechnol.* **35**, 1179–1187 (2017).
50. L. Cong, F. A. Ran, D. Cox, S. Lin, R. Barretto, N. Habib, P. D. Hsu, X. wu, W. Jiang, L. A. Marraffini, F. Zhang, Multiplex genome engineering using CRISPR/Cas systems. *Science* **339**, 819–823 (2013).
51. J. A. Zepp, W. J. Zacharias, D. B. Frank, C. A. Cavanaugh, S. Zhou, M. P. Morley, E. E. Morrisey, Distinct mesenchymal lineages and niches promote epithelial self-renewal and myofibrogenesis in the lung. *Cell* **170**, 1134–1148.e10 (2017).
52. Y. Wang, D. B. Frank, M. P. Morley, S. Zhou, X. Wang, M. M. Lu, M. A. Lazar, E. E. Morrisey, HDAC3-dependent epigenetic pathway controls lung alveolar epithelial cell remodeling and spreading via miR-17-92 and TGF-β signaling regulation. *Dev. Cell* **36**, 303–315 (2016).

Acknowledgments: We thank the Flow Cytometry Core at the CHOP and the Histology, Gene Expression, and Microscopy Cores at the University of Pennsylvania for help in performing the studies. The PX458 and PX330 plasmids were obtained from Addgene and are gifts from F. Zhang. **Funding:** E.E.M. is supported by funding from the NIH (HL134745 and HL132999). W.H.P. is supported by funding from the National Center for Advancing Translational Sciences of the NIH and the Institute for Translational Medicine and Therapeutics at the University of Pennsylvania (UL1-TR001878), the Orphan Disease Center at the University of Pennsylvania (GE-16-001-IU), and gifts to the Children's Hospital of Philadelphia. M.F.B. is supported by funding from the NIH (HL119436), the U.S. Department of Veterans Affairs (VA Merit Review 1I01BX001176), and the Pulmonary Fibrosis Foundation. J.K. was supported by NIH 2 T32 HL007586. D.A. is supported by The Nemours Foundation. **Author contributions:** D.A., W.J.Z., M.F.B., E.E.M., and W.H.P designed the experiments and wrote the manuscript. D.A., W.J.Z., H.A.H., A.C.R., J.D.S., N.J.A., S.Z., H.L., J.K., Y.T., J.M., A.C.C., K.S., B.C., and W.H.P. performed experiments and analyzed data. K.M. analyzed bioinformatics data of off-target effects. **Competing interests:** A.C.C. is currently an employee of Endcardia Inc. The other authors declare that they have no competing interests. **Data and materials availability:** All data associated with this study are present in the paper or the Supplementary Materials. DNA sequencing data have been deposited on the NCBI Sequence Read Archive under accession no. PRJNA505864.

Submitted 24 October 2018
Accepted 3 January 2019
Published 17 April 2019
10.1126/scitranslmed.aav8375

Citation: D. Alapati, W. J. Zacharias, H. A. Hartman, A. C. Rossidis, J. D. Stratigis, N. J. Ahn, B. Coons, S. Zhou, H. Li, K. Singh, J. Katzen, Y. Tomer, A. C. Chadwick, K. Musunuru, M. F. Beers, E. E. Morrisey, W. H. Peranteau, In utero gene editing for monogenic lung disease. *Sci. Transl. Med.* **11**, eaav8375 (2019).

Science Translational Medicine

In utero gene editing for monogenic lung disease

Deepthi Alapati, William J. Zacharias, Heather A. Hartman, Avery C. Rossidis, John D. Stratigis, Nicholas J Ahn, Barbara Coons, Su Zhou, Hiaying Li, Kshitiz Singh, Jeremy Katzen, Yaniv Tomer, Alexandra C. Chadwick, Kiran Musunuru, Michael F. Beers, Edward E. Morrisey and William H. Peranteau

Sci Transl Med **11**, eaav8375.
DOI: 10.1126/scitranslmed.aav8375

Editing out a lethal lung disease

Surfactant, a lipoprotein mixture that reduces lung surface tension, is essential for normal lung function. In rare cases, infants are born with genetic surfactant deficiency, resulting in rapid death from respiratory failure. Because of the immediate perinatal fatality associated with this disease, any effective intervention would need to be applied before delivery. Alapati *et al*. used a mouse model of genetic surfactant deficiency to demonstrate the feasibility of in utero gene editing to delete the mutant allele. The authors showed that correction of the genetic defect before birth improved lung development and survival in the treated animals, demonstrating the feasibility of this therapeutic intervention.